

Evgeni Fedorovich*, Robert Conzemius, and Alan Shapiro
School of Meteorology, University of Oklahoma, Norman, Oklahoma

1. INTRODUCTION

Development of convective boundary layer in a uniformly stratified, shear-free atmosphere has been extensively studied experimentally, both in the laboratory and in nature (see, e.g., Deardorff et al. 1980, Boers and Eloranta 1986, Nelson et al. 1989), by means of bulk models of differing complexity (see, e.g., Tennekes 1973, Zilitinkevich 1991, van Zanten et al. 1999, Fedorovich and Mironov 1995), and, most extensively, though numerical large eddy simulations (LES; see, e.g., Deardorff 1974, Lewellen and Lewellen 1998, Sullivan et al. 1998, Lock and MacVean 1999, Fedorovich et al. 2004). It has been established that at times long enough for the CBL structure to forget about initial conditions, the boundary layer growth happens in an equilibrium (quasi-stationary) manner, with the convective entrainment – which is a driving mechanism of the CBL development – being controlled by the balance between the buoyancy energy supply from the underlying surface and the energy dissipation in the bulk of the CBL. This balance leads to the CBL depth increasing as a function of the square-root of time. This behavior can be vividly illustrated in terms of the so-called zero-order model (ZOM) of entrainment introduced by Lilly (1968) and reevaluated against LES data in Fedorovich et al. (2004).

The ZOM approximates the horizontally averaged profile of buoyancy in the CBL as a function of height with a zero-order discontinuity in place of the capping inversion layer. An important hypothesis underlying the ZOM in this case is the instantaneous adjustment of the CBL turbulence structure to the integral parameters of the layer. It is assumed, for instance, that appropriately scaled profiles of turbulence kinetic energy (TKE) and its dissipation rate integrate to universal constants over the layer. Experimental and numerical data obtained to date generally support these assumptions.

The present study is concerned with the extent to which the above assumptions are valid when the growing CBL encounters a discontinuity (or heterogeneity) in the stratification of the free atmosphere (a situation much more realistic than the stratification uniformity). Does the CBL turbulence regime instantly adjust to the stratification change? Can convective entrainment still be regarded as a quasi-stationary process? How does the CBL depth change with time after the layer proceeds into the new environment, and how long does it take for the CBL to adjust to the new outer stratification?

We address these issues by applying LES to (i) the shear-free CBL that grows initially in a relatively weakly

stratified atmosphere, with subsequent change to a stronger stratification, and (ii) to the inverse situation, when the CBL passes through an abrupt change from stronger to weaker stratification. We then apply the ZOM formalism to analyze and interpret the numerical simulation data.

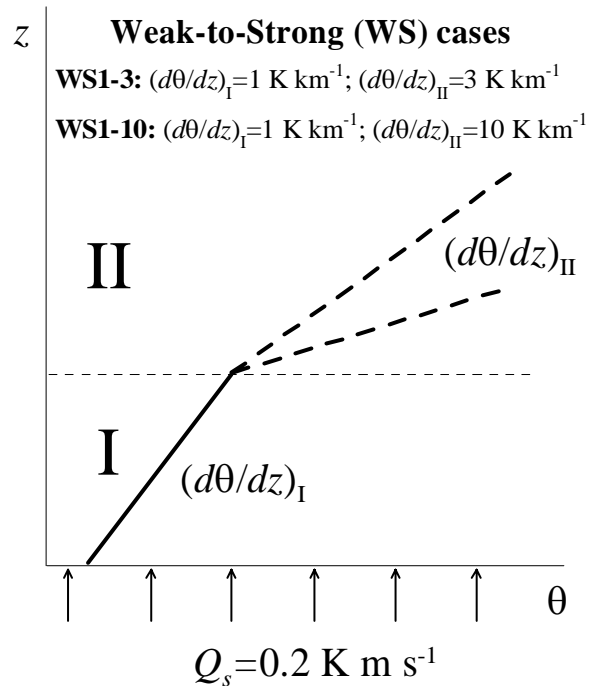


Figure 1. Schematics of initial profiles of the virtual potential temperature θ corresponding to the CBL growth first through a weakly stratified atmosphere (I) with the change to a strongly stratified atmosphere (II).

2. SIMULATION SETUP

For numerical simulations of entrainment, we used the LES code of Fedorovich et al. (2001, 2004). This code employs a finite-difference spatial discretization of filtered equations of atmospheric dynamics and thermodynamics, and the leap-frog scheme with a weak Asselin filter for the time advancement. For the subgrid turbulence parameterization, the Deardorff (1980) closure, which is based on a prognostic equation for the subgrid turbulence kinetic energy, is used. The pressure is calculated diagnostically from the Poisson equation solved by combining the Fast Fourier Transform technique in the x and y directions and a tri-diagonal matrix inversion over z . Monin-Obukhov similarity

relationships are applied locally across the first mesh layer at the surface to relate the one-point dynamic and thermal parameters of the flow near the wall. The simulations were run in the domain of $x \times y \times z = 8 \text{ km} \times 8 \text{ km} \times 4 \text{ km}$ with periodic lateral boundary conditions, on a $200 \times 200 \times 100$ staggered grid with uniform spacing of $\Delta x = \Delta y = \Delta z = 40 \text{ m}$.

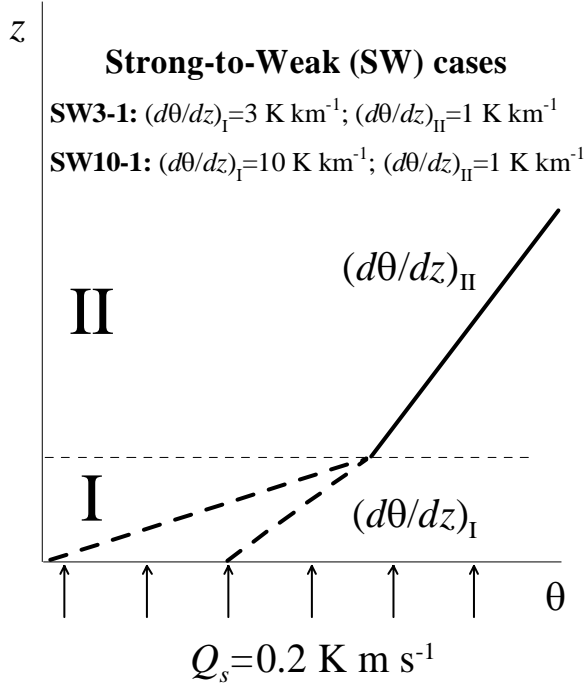


Figure 2. Same as in Fig. 1, but for the CBL initial growth through a strongly stratified atmosphere (I), with the change to a weakly stratified atmosphere (II).

Initial (virtual potential) temperature profiles for the simulated CBL cases, which correspond to the stratification change from weak to strong (**WS** cases) and strong to weak (**SW** cases), are schematically shown in Figs. 1 and 2. For reference, three cases of CBL evolving in a uniformly stratified atmosphere with height-constant temperature gradients of 1 K km^{-1} (**UNI1** case), 3 K km^{-1} (**UNI3** case), and 10 K km^{-1} (**UNI10** case) were simulated (not shown in Figs. 1 and 2). These gradients correspond to the interval gradients used in the cases with heterogeneous stratification (**WS1-3**, **WS1-10**, **SW3-1**, and **SW10-1**, see Figs. 1 and 2).

The same values of virtual potential temperature flux at the surface, $Q_s = 0.2 \text{ K m s}^{-1}$, and surface roughness $Z_0 = 0.01 \text{ m}$ were prescribed in all simulated CBL cases. Turbulent convection was initiated by random temperature perturbations in the first grid-cell layer adjacent to the surface at the first time step of the simulation.

Turbulence statistics were calculated by averaging (denoted hereafter by overbar) over the horizontal planes only, without complementary time averaging.

The CBL depth z_i was determined from profiles of the total (resolved + subgrid) kinematic heat flux $\overline{w'\theta'}$ (at the surface, it is equal to Q_s) by taking z_i as the height of the heat flux minimum within the entrainment zone. Profiles of the turbulence kinetic energy (TKE), e , were calculated by summing the total velocity variances and dividing the result by 2. The TKE dissipation rate ε was evaluated from the employed subgrid turbulence model.

3. CBL EVOLUTION IN AN ATMOSPHERE WITH UNIFORM STRATIFICATION

The CBL depth as function of time for the cases with uniform stratification of the atmosphere above the CBL (cases **UNI1**, **UNI3**, and **UNI10**) is shown in Fig. 3. As demonstrated in Fedorovich et al. (2004), in these cases, the entrainment reaches an equilibrium regime after a certain time into simulation. A ZOM expression for the CBL depth evolution in this regime reads

$$z_i = [2(1 + 2C_1)B_s t]^{1/2} N^{-1}, \quad (1)$$

where $B_s = (g/\theta_0)Q_s$ is the surface buoyancy flux (g is the gravitational acceleration, θ_0 is the reference temperature), $N = [(g/\theta_0)(d\theta/dz)]^{1/2}$ is the Brunt-Väisälä (buoyancy) frequency in the free atmosphere above the CBL, and C_1 is the empirical constant representing the ZOM entrainment heat flux ratio in the equilibrium entrainment regime. The $z_i(t)$ data in Fig. 3 reveals a good agreement between the LES predictions and the analytical ZOM solution (1) with the commonly adopted value of $C_1 = 0.2$ (Zilitinkevich 1991).

In the ZOM of the entraining CBL, the TKE balance equation, integrated over the CBL depth, takes on the following form (Fedorovich et al. 2004):

$$\frac{d}{dt} \int_0^{z_i} e dz = \frac{z_i}{2} \left(B_s - \Delta b \frac{dz_i}{dt} \right) - \Phi_i - \int_0^{z_i} \varepsilon dz, \quad (2)$$

where Φ_i stands for the upward energy flux at the CBL top and $\Delta b = (g/\theta_0)\Delta\theta$ is the buoyancy jump across the inversion layer represented in the ZOM by a discontinuity interface. The assumption is further made that the TKE and its dissipation rate can be parameterized as

$$e = w_*^2 \varphi_e(z/z_i) \quad \text{and} \quad \varepsilon = \frac{w_*^3}{z_i} \varphi_\varepsilon(z/z_i), \quad (3)$$

with universal functions φ_e and φ_ε that integrate to universal constants $C_e = \int_0^1 \varphi_e(\zeta) d\zeta$ and

$C_\varepsilon = \int_0^1 \varphi_\varepsilon(\zeta) d\zeta$. This assumption is based on the Zilitinkevich and Deardorff (1974) hypothesis of self-similarity of the CBL turbulence regime in the process of the CBL evolution, when z_i and $w_* = (z_i B_s)^{1/3}$ – the so-called convective velocity scale – are both changing with time. In other words, the CBL turbulence quantities are expected to adjust to the CBL evolution through z_i , which is the integral parameter of the layer (the value of surface buoyancy flux B_s is considered constant in our study).

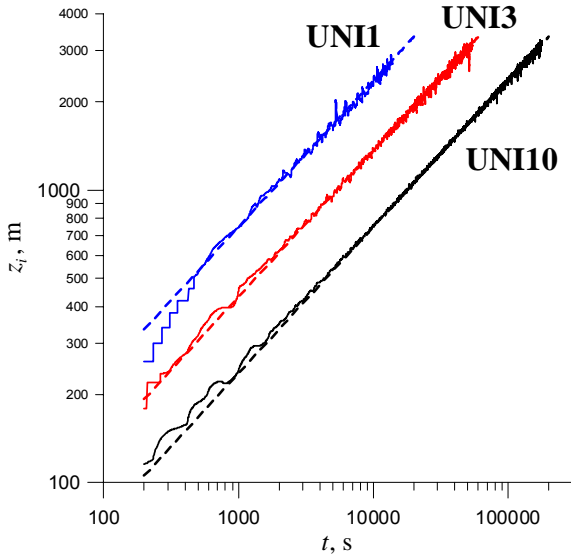


Figure 3. Simulated CBL depth evolution in the cases with uniform free-atmosphere stratification. The straight dashed lines show the ZOM solutions with $C_1=0.2$.

In the equilibrium entrainment regime, the left-hand side of (2) and the energy flux term on the right-hand side vanish, and, with due account to the employed scaling of ε , the integral TKE balance equation reduces to

$$\frac{\Delta b(dz_i / dt)}{B_s} = 1 - 2C_\varepsilon \equiv C_1, \quad (4)$$

from which the physical meaning of C_1 becomes clear.

It is possible to notice, however, that the parameterizations (3) for e and ε do not include any explicit dependence on the free-atmosphere stratification and thus, the integral parameters C_e and C_ε are considered to be independent, not only of time, but also of N . One insufficiency of the Zilitinkevich and Deardorff (1974) scaling is rather well known (see, e.g., Sorbjan 1996): the scaled turbulence statistics in the CBL usually show better universal behavior in the lower portion of the CBL than in the upper part of the layer,

where the influence of the capping inversion becomes important.

How significantly do the e and ε integrals vary with the outer flow stratification in the simulated CBL cases? Time dependencies of the normalized integrals of e and ε , evaluated as

$$I_{ne} = \frac{1}{z_i w_*^2} \int_0^\infty e dz \quad \text{and} \quad I_{n\varepsilon} = \frac{1}{w_*^3} \int_0^\infty \varepsilon dz, \quad (5)$$

are shown in Fig. 4.

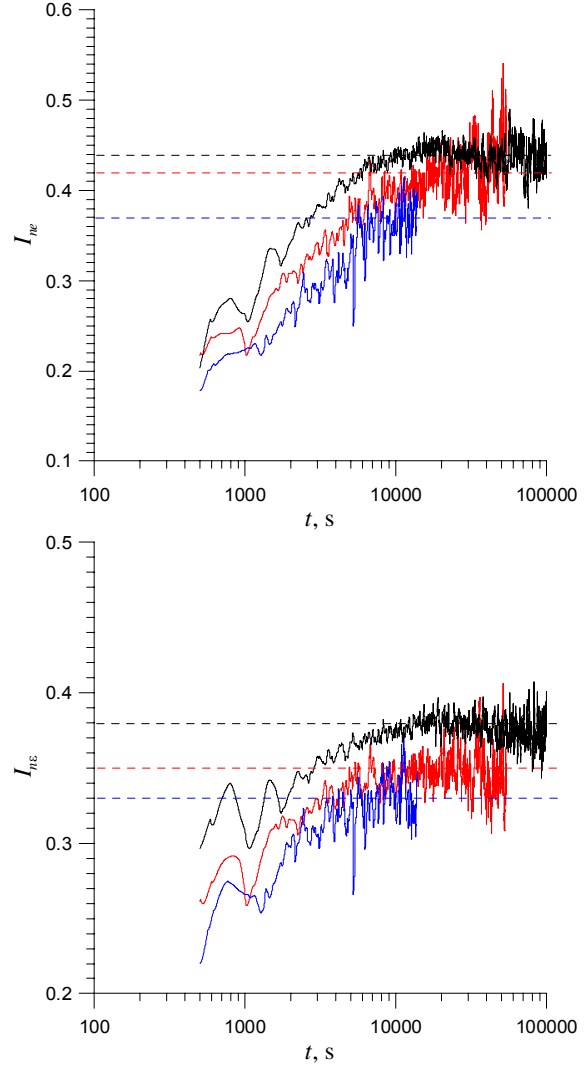


Figure 4. Time evolution of the normalized integrals of e (upper plot) and ε (lower plot) in the UNI1 (blue), UNI3 (red), and UNI10 (black) cases.

The LES data indicate that integrals of TKE and its dissipation rate in the equilibrium entrainment regime are indeed quasi-independent of time (in this sense, they are close to constants C_e and C_ε), but show a noticeable (although weak) dependence on the free-

atmosphere stratification. Namely, the values of both integrals increase slightly with N . Nevertheless, with a certain degree of approximation, turbulence regimes in the simulated CBLs at the equilibrium stages of their evolution may be considered self-similar. At the same time, the simulation data in Figs. 3 and 4 confirm the applicability of (4) and thus, the insensitivity of the CBL growth rate at large t to the integral value of TKE (or constant C_ϵ) as long as it remains reasonably small.

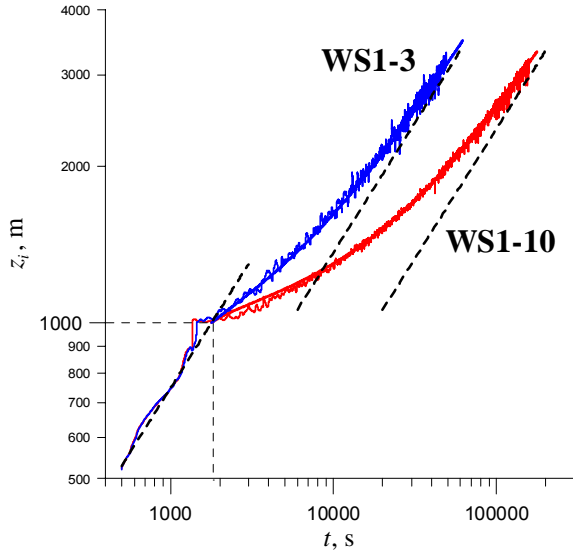


Figure 5. Evolution of the CBL depth in the heterogeneously stratified atmosphere with stratification changing from weak to strong (Fig. 1). Simulated $z_i(t)$ are shown by thin irregular lines, blue for the **WS1-3** case and red for the **WS1-10** case. Solid curves of respective color show non-stationary ZOM solutions for both cases in the post-transition time. Straight dashed lines present the ZOM equilibrium solutions (with $C_1=0.2$) for stratifications 1 K km^{-1} , 3 K km^{-1} , and 10 K km^{-1} (from left to right).

The smaller values of I_{ne} in Fig. 4 compared to the commonly accepted value of $C_\epsilon=0.4$ (which corresponds to $C_1=0.2$) may be a result of differences in the integral evaluation procedures and of the spurious damping of small-scale fluctuations of the resolved velocity in the employed LES code (it leads to smaller values of subgrid TKE and, consequently, to smaller dissipation values). On the other hand, the numerical damping in the code also attenuates the energy available for entrainment, so its net effect on the entrainment and CBL growth, as one may conclude from Fig. 3, turns out to be close to zero.

One may see that the integrals of both e and ϵ in Fig. 4 change rather significantly before the CBL reaches the equilibrium state. This observation makes the applicability of the concept of self-similarity of the

CBL turbulence structure to non-stationary stages of the CBL evolution rather questionable.

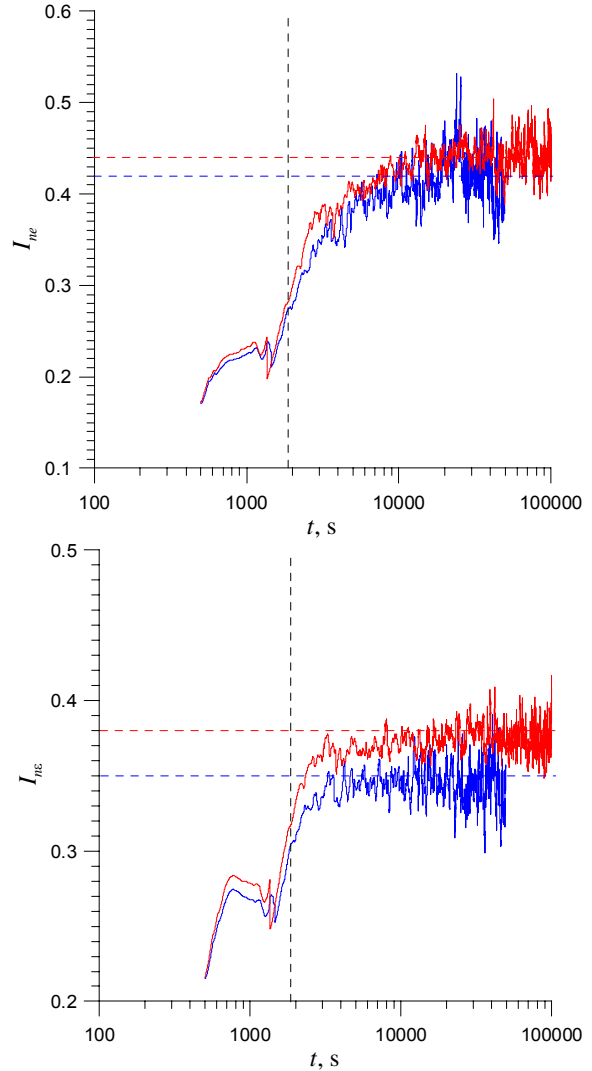


Figure 6. Time evolution of the normalized integrals of e (upper plot) and ϵ (lower plot) in the **WS1-3** (blue), and **WS1-10** (red) cases. Vertical dashed lines correspond to the moment of the passage of the CBL top through the stratification change. Horizontal dashed lines show equilibrium values of corresponding integrals in the **UNI3** and **UNI10** cases (see Fig. 4).

4. CBL EVOLUTION IN ATMOSPHERES WITH HETEROGENEOUS STRATIFICATION

We first consider characteristics of the CBL evolution in the **WS** cases sketched in Fig. 1. Time dependencies of the CBL depth for these cases are illustrated in Fig. 5. In both simulated cases, the change from weak to strong stratification happens at $z=1000 \text{ m}$, which is approximately 1800 s into simulation. Prior to this moment, $z_i(t)$ follows reasonably well the ZOM prediction for the equilibrium CBL growth in the

atmosphere with a temperature gradient of 1 K km^{-1} . Note, however, that the turbulence regime of the CBL at this time (see **UNI1** curves in Fig. 4) has not yet reached equilibrium.

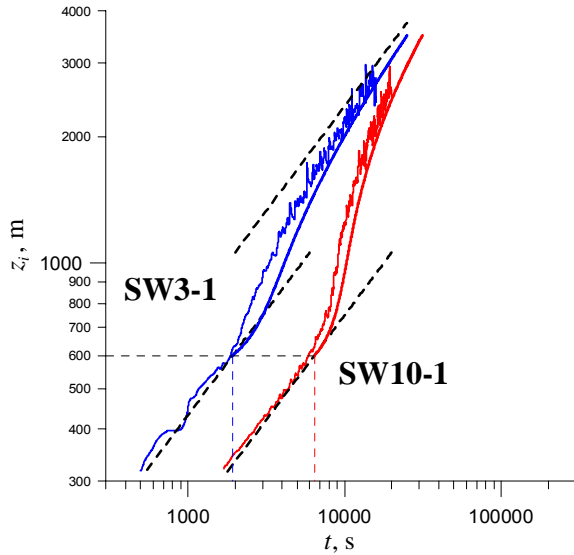


Figure 7. Evolution of the CBL depth in the heterogeneously stratified atmosphere with stratification changing from strong to weak (Fig. 2). Simulated $z_i(t)$ are shown by thin irregular lines, blue for the **SW3-1** case and red for the **SW10-1** case. Solid curves of respective color show non-stationary ZOM solutions for both cases in the post-transition time. Straight dashed lines present the ZOM equilibrium solutions (with $C_1=0.2$) for stratifications 1 K km^{-1} , 3 K km^{-1} , and 10 K km^{-1} (from left to right).

When the CBL top reaches the stratification change elevation, its growth considerably slows down. In the **WS1-10** case of very strong new stratification, the growth actually stalls for some time. At this stage, in both cases, changes of z_i with time look very different from its behavior in the equilibrium entrainment regime. The CBL adjustment to new conditions requires a lot of time, even in the **WS1-3** case, where the upper stratification is weaker. Needless to say, in both cases, the complete adjustment is not achieved on the time scales comparable with time scales of the CBL daytime evolution.

Time changes of the e and ε integrals (5), shown in Fig. 6, demonstrate the evolution of the CBL turbulence parameters corresponding to the CBL development in the **WS** cases. First of all, it is clear that in both cases, the change to the new stronger stratification boosts the growth of integral TKE and dissipation, and in the case with the strongest new stratification, this growth is considerably faster. The dissipation integrals grow faster than the TKE integrals at the first stages of the CBL transition to the new atmospheric stratification. Later, however, the growth of the dissipation integrals slows down, and both integrals

reach equilibrium values for the new stratification over approximately the same time. In qualitative agreement with the $z_i(t)$ behavior (Fig. 6), these equilibrium values are reached earlier in the **WS1-3** case than in the **WS1-10** case. Nevertheless, in both cases, the evolution of the CBL depth is still far from its equilibrium behavior, even when the TKE and dissipation integrals have already reached their equilibrium values.

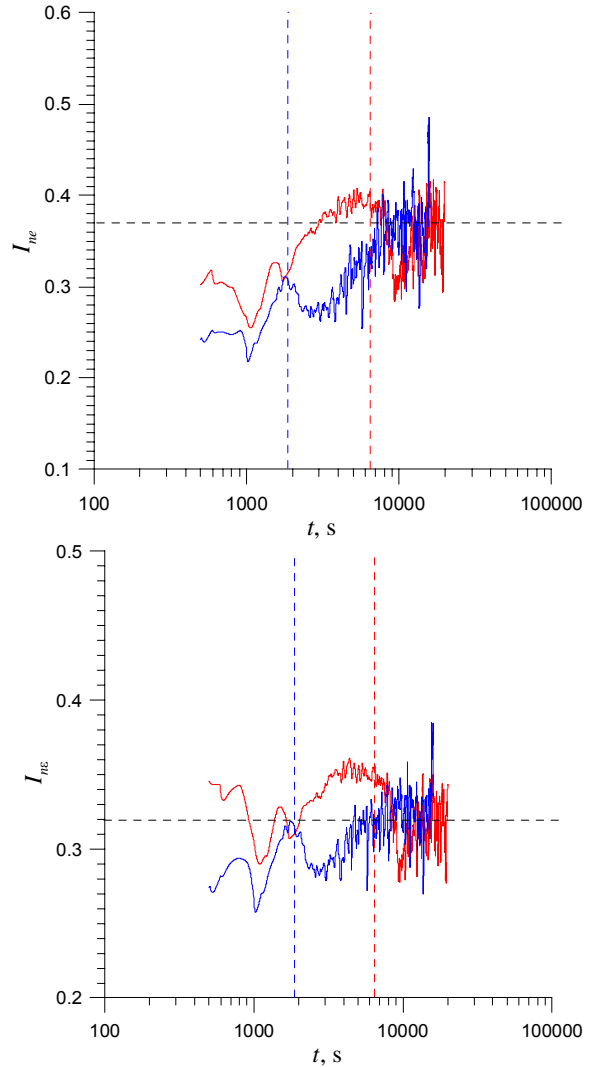


Figure 8. Time evolution of the normalized integrals of e (upper plot) and ε (lower plot) in the **SW3-1** (blue), and **SW10-1** (red) cases. Vertical dashed lines correspond to the moment of the passage of the CBL top through the stratification change. Horizontal dashed line shows equilibrium values of corresponding integrals in the **UNI1** case (see Fig. 4).

Plots of the CBL depth evolution in the **SW** cases are presented in Fig. 7. In both cases shown, the CBL transition to the new atmospheric stratification happens at the same height (600 m), but in the **SW10-1** case of stronger initial stratification the start of transition is

considerably delayed compared to the weaker-stratification case **SW3-1**. Changes of the CBL depth with time in the post-transition period are rather fast in the **SW** cases. For instance, in the **SW10-1** case, the CBL depth jumps from 600 m to 1000 m in a matter of minutes. Evolution of the turbulence regime parameters corresponding to these rapid changes of the CBL vertical extension are shown in Fig. 8. The observed changes of the TKE and dissipation integrals in the post-transition time intervals point to the strong non-stationarity of the turbulence regime in the rapidly expanding CBL. Immediately (or shortly after) the CBL passes the stratification change elevation, the values of both integrals diminish to values much smaller than their equilibrium values for the upper stratification, and it takes some time for them to recover. However, like in the **WS** cases, even after the integrals reach their equilibrium values, the CBL depth still does not follow the equilibrium solution.

5. INTERPRETATION OF RESULTS IN TERMS OF ZERO-ORDER ENTRAINMENT MODEL

Let us now analyze the CBL development in a heterogeneous atmosphere using the ZOM conceptual framework. We apply the integral TKE balance equation (2), omitting the energy transport term (which is small within the considered stratification range),

$$\frac{d}{dt} \int_0^{z_i} \epsilon dz = \frac{z_i}{2} \left(B_s - \Delta b \frac{dz_i}{dt} \right) - \int_0^{z_i} \epsilon dz, \quad (6)$$

and we also employ the ZOM equation of the CBL integral heat balance (Zilitinkevich 1991):

$$\frac{d}{dt} \left(\frac{N^2 z_i^2}{2} - z_i \Delta b \right) = B_s. \quad (7)$$

By approximating the integrals in (6) through $I_{ne}(t)$ and $I_{n\epsilon}(t)$ given by (5), we come to the following entrainment-rate equation:

$$\frac{dz_i}{dt} = \frac{1 - 2I_{n\epsilon} - \frac{2z_i}{w_*} \frac{dI_{ne}}{dt}}{\frac{10}{3} \frac{I_{ne}}{w_*} + \frac{\Delta b}{B_s}}. \quad (8)$$

Introducing in (7) and (8) normalized variables $x = z_i B_s^{-1/2} N^{3/2}$, $y = \Delta b B_s^{-1/2} N^{-1/2}$ and $\tau = tN$ after Zilitinkevich (1991), we obtain the following system of ordinary differential equations:

$$\frac{dx}{d\tau} = \frac{1 - 2I_{n\epsilon} - 2x^{2/3} \frac{dI_{ne}}{d\tau}}{\frac{10}{3} \frac{I_{ne}}{x^{1/3}} + y}. \quad (9)$$

$$\frac{d}{d\tau} \left(\frac{x^2}{2} - xy \right) = 1. \quad (10)$$

With the integral turbulence parameters in (9) taken constant, $I_{ne} = C_e$ and $I_{n\epsilon} = C_\epsilon$, as suggested by the Zilitinkevich and Deardorff (1974) scaling, (9) becomes

$$\frac{dx}{d\tau} = \frac{C_1}{\frac{C_2}{x^{1/3}} + y}, \quad (11)$$

where $C_2 = C_e / 0.3$ and $C_1 = 1 - 2C_\epsilon$ (see also Eq. 4). Equations (10) and (11), complemented with initial conditions $x(\tau_0) = x_0$ and $y(\tau_0) = y_0$, have the following analytical solution:

$$\tau = \frac{1}{2C_1(2+1/C_1)} \left[1 - \left(\frac{x_0}{x} \right)^{2+1/C_1} \right] x^2 + \frac{C_2}{C_1(2/3+1/C_1)} + \left[1 - \left(\frac{x_0}{x} \right)^{2/3+1/C_1} \right] x^{2/3} + x_0 \left(y_0 - \frac{x_0}{2} \right) \left[1 - \left(\frac{x_0}{x} \right)^{1/C_1} \right] + t_0, \quad (12)$$

$$y = \frac{1}{2+1/C_1} \left[1 - \left(\frac{x_0}{x} \right)^{2+1/C_1} \right] x + y_0 \left(\frac{x_0}{x} \right)^{1+1/C_1} - \frac{C_2}{C_1(2/3+1/C_1)} \left[1 - \left(\frac{x_0}{x} \right)^{2/3+1/C_1} \right] x^{-1/3}. \quad (13)$$

This analytical solution with $C_1 = 0.2$ and $C_2 = 4/3$ was tested against the LES predictions of the post-transition CBL growth for all four cases with heterogeneous stratification (**WS1-3**, **WS1-10**, **SW3-1**, and **SW10-1**). The results for z_i are presented in Figs. 5 and 7. The values of constants in (10) and (11) were chosen based on the empirical C_e and C_ϵ data summarized in Zilitinkevich (1991) and the LES estimates of the average values of I_{ne} and $I_{n\epsilon}$ in the equilibrium entrainment regime (see Figs. 6 and 8).

Comparison of the analytical and numerical predictions of $z_i(t)$ for the **WS** cases (Fig. 5) shows that in these cases the CBL in the post-transition phase indeed develops in a quasi-stationary manner and its turbulence regime can be considered as approximately self-similar. Despite the fact that local changes of $z_i(t)$ in time under such conditions can considerably differ from the 1/2 power law characteristic of the equilibrium evolution, the overall changes of CBL depth are described rather decently by the ZOM based on the

scaling concept of Zilitinkevich and Deardorff (1974), which implies self-similarity of turbulence regime in the evolving CBL. We also found that under such conditions the behavior of $z_i(t)$ is primarily determined by the initial values of z_i and Δb , and by the dissipation integral (C_ε), while the sensitivity of solution to the value of C_ε is rather weak.

However, in the cases of fast CBL evolution during its transition to the weakly stratified environment (**SW** cases), the ZOM solutions with chosen values of constants do not match LES predictions of $z_i(t)$ as nicely as in **WS** cases. Attempted variation of C_ε and C_ε values within reasonable limits did not provide any better agreement between the analytical and numerical $z_i(t)$ predictions in Fig. 7. Apparently, under these conditions the CBL turbulence regime is not self-similar in the Zilitinkevich and Deardorff (1974) sense, and the ZOM analysis should be based on Eq. (9), which includes integral parameters I_{ne} and I_{nc} dependent on time, rather than on Eq. (11) with universal constants.

Some of observed features of the simulated z_i evolution (Fig. 7) as related to the time changes of I_{ne} and I_{nc} (Fig. 8) can be readily explained in terms of (9). For instance, it follows from (9) that in the **SW** cases smaller values of I_{ne} (in the denominator) along with smallness of I_{nc} and negative sign of dI_{ne}/dt (in the numerator) – all together contribute to fast z_i post-transition growth observed in Fig. 7.

6. SUMMARY AND CONCLUSIONS

In the reported LES experiments we have reproduced two types of the CBL evolution in a heterogeneously stratified atmosphere.

In the first set of simulated cases (**WS**), the CBL growth was slowed down by the strongly stratified environment, and the turbulence regime was gradually adjusting to this new environment. The zero-order model (ZOM) of entrainment, with conventional values of universal constants resulting from self-similarity assumptions, was found to describe the simulated CBL evolution rather well in these cases.

In the second group of experiments (**SW**), we studied the opposite type of CBL, which proceeded in its development from a strongly to a weakly stratified environment. These cases were characterized by strong non-stationarity of the CBL evolution. In order to adequately reproduce the CBL growth under these conditions by the ZOM, the model should directly take into account the non-stationarity of the CBL turbulence structure.

Acknowledgement: Authors gratefully acknowledge support by National Science Foundation (grant ATM-0124068).

- Boers, R., and E. W. Eloranta, 1986: Lidar measurements of the atmospheric entrainment zone and the potential temperature jump across the top of the mixed layer. *Bound.-Layer Meteor.*, **34**, 357-375.
- Deardorff, J. W., 1974: Three dimensional numerical study of turbulence in an entraining mixed layer. *Bound.-Layer Meteor.*, **7**, 199-226.
- Deardorff, J. W., G. E. Willis, and B. H. Stockton, 1980: Laboratory studies of the entrainment zone of a convectively mixed layer. *J. Fluid Mech.*, **100**, 41-64.
- Deardorff, J. W., 1980: Stratocumulus-capped mixed layers derived from a three-dimensional model. *Bound.-Layer Meteor.*, **18**, 495-527.
- Fedorovich, E., R. Conzemius, and D. Mironov, 2004: Convective entrainment into a shear-free linearly stratified atmosphere: bulk models reevaluated through large eddy simulations. *J. Atmos. Sci.*, **61**, 281-295.
- Fedorovich, E., F. T. M. Nieuwstadt, and R. Kaiser, 2001: Numerical and laboratory study of horizontally evolving convective boundary layer. Part I: Transition regimes and development of the mixed layer. *J. Atmos. Sci.*, **58**, 70-86.
- Lewellen D. C., and W. S. Lewellen, 1998: Large-eddy boundary layer entrainment. *J. Atmos. Sci.*, **55**, 2645-2665.
- Lilly, D. K., 1968: Models of cloud-topped mixed layers under a strong inversion. *Quart. J. Roy. Meteorol. Soc.*, **94**, 292-309.
- Lock, A. P., and M. K. MacVean, 1999: A parameterisation of entrainment driven by surface heating and cloud-top cooling. *Quart. J. Roy. Meteor. Soc.*, **125**, 271-300.
- Nelson, E., R. Stull, and E. Eloranta, 1989: A prognostic relationship for entrainment zone thickness. *J. Appl. Meteorol.*, **28**, 885-903.
- Sorbjan, Z., 1996: Effects caused by varying the strength of the capping inversion based on a large eddy simulation model of the shear-free convective boundary layer. *J. Atmos. Sci.*, **53**, 2015-2024.
- Sullivan, P., C.-H. Moeng, B. Stevens, D. H. Lenschow, and S. D. Mayor, 1998: Structure of the entrainment zone capping the convective atmospheric boundary layer. *J. Atmos. Sci.*, **55**, 3042-3064.
- Tennekes, H., 1973: A model for the dynamics of the inversion above a convective boundary layer. *J. Atmos. Sci.*, **30**, 558-567.
- van Zanten, M. C., P. G. Duynkerke, and J. W. M. Cuijpers, 1999: Entrainment parameterization in convective boundary layers derived from large eddy simulations. *J. Atmos. Sci.*, **56**, 813-828.
- Zilitinkevich, S. S., 1991: *Turbulent Penetrative Convection*. Avebury Technical, Aldershot, 179 pp.
- Zilitinkevich, S. S., and J. W. Deardorff, 1974: Similarity theory for the planetary boundary layer of time-dependent height. *J. Atmos. Sci.*, **31**, 1449-1452.